

Neuronal Excitability

Selective Overexpression of Collybistin in Mouse Hippocampal Pyramidal Cells Enhances GABAergic Neurotransmission and Protects against PTZ-Induced Seizures

Shanu George, Shaun James, and Angel L. De Blas

<https://doi.org/10.1523/ENEURO.0561-20.2021>

Department of Physiology and Neurobiology, University of Connecticut, Storrs, CT 06269

Abstract

Collybistin (CB) is a rho guanine exchange factor found at GABAergic and glycinergic postsynapses that interacts with the inhibitory scaffold protein, gephyrin, and induces accumulation of gephyrin and GABA type-A receptors (GABA_ARs) to the postsynapse. We have previously reported that the isoform without the src homology 3 (SH3) domain, CBSH3⁻, is particularly active in enhancing the GABAergic postsynapse in both cultured hippocampal neurons as well as in cortical pyramidal neurons after chronic *in vivo* expression in *in utero* electroporated (IUE) rats. Deficiency of CB in knock-out (KO) mice results in absence of gephyrin and gephyrin-dependent GABA_ARs at postsynaptic sites in several brain regions, including hippocampus. In the present study, we have generated an adeno-associated virus (AAV) that expresses CBSH3⁻ in a cre-dependent manner. Using male and female VGLUT1-IRES-cre or VGAT-IRES-cre mice, we explore the effect of overexpression of CBSH3⁻ in hippocampal pyramidal cells or hippocampal interneurons. The results show that: (1) the accumulation of gephyrin and GABA_ARs at inhibitory postsynapses in hippocampal pyramidal neurons or interneurons can be enhanced by CBSH3⁻ overexpression; (2) overexpression of CBSH3⁻ in hippocampal pyramidal cells can enhance the strength of inhibitory neurotransmission; and (3) these enhanced inhibitory synapses provide protection against pentylenetetrazole (PTZ)-induced seizures. The results indicate that this AAV vector carrying CBSH3⁻ can be used for *in vivo* enhancement of GABAergic synaptic transmission in selected target neurons in the brain.

Key words: AAV; collybistin; GABA; gephyrin; PTZ

Significance Statement

Excessive or imbalanced excitation in the hippocampus can result in acute or chronic pathologic conditions, such as seizures, epilepsy, and learning impairments. It is therefore important to uncover target genes that can be manipulated to restore or prevent this imbalance. This study uses a novel adeno-associated virus (AAV) to express collybistin (CB)SH3⁻ in select cells of the hippocampus. We have found that overexpression of this protein enhances GABAergic inhibitory synaptic transmission. The results also bring attention to CB as a possible target for therapeutic intervention aimed to restore the balance between excitation and inhibition.

Received December 27, 2020; accepted May 23, 2021; First published June 3, 2021.

The authors declare no competing financial interests.

Author contributions: S.G. and A.L.D. designed research; S.G. and S.J. performed research; S.G. and S.J. analyzed data; S.G., S.J., and A.L.D. wrote the paper.

Introduction

Phasic inhibitory neurotransmission in the central nervous system is accomplished through the action of the neurotransmitters GABA or glycine acting on ligand-gated channels which primarily cluster at postsynaptic sites. GABA type-A receptors (GABA_ARs) concentrate at postsynaptic sites through interactions with postsynaptic proteins, including anchoring on the inhibitory scaffolding protein, gephyrin (Kneussel et al., 1999; Tretter et al., 2008, 2011; Saiepour et al., 2010; Mukherjee et al., 2011). Collybistin (CB) is a guanine exchange factor that interacts with gephyrin, inducing the recruitment of gephyrin and CB, itself, to GABAergic postsynapses (Kins et al., 2000; Grosskreutz et al., 2001; Reddy-Alla et al., 2010). Rodents express several isoforms of CB that differ in C termini (CB1, CB2, CB3), but can also either possess or lack a regulatory src homology 3 (SH3) domain (Kins et al., 2000; Harvey et al., 2004). Isoforms that possess the SH3 domain (CBSH3+) are in an auto-inhibited conformation, thus preventing the pleckstrin homology (PH) domain of CBSH3+ from binding to phosphoinositides of the neuronal membrane (Soykan et al., 2014; Papadopoulos et al., 2015; Ludolphs et al., 2016) unless auto-inhibition is removed through the binding of neuroligin-2 (NL2) or GABA_AR subunit- α 2 to the SH3 domain, or the small GTPase, TC10, to the PH domain (Poulopoulos et al., 2009; Saiepour et al., 2010; Mayer et al., 2013; Papadopoulos et al., 2017; Nathanson et al., 2019). Isoforms that lack the SH3 domain (CBSH3-), are not constrained in this fashion, inducing the formation of submembranous gephyrin clusters, as demonstrated in HEK and COS-7 cells (Kins et al., 2000; Harvey et al., 2004; Poulopoulos et al., 2009).

Studies of CB knock-out (KO) mice reveal that loss of CB results in severe disruption to clustering of gephyrin and GABA_ARs in certain brain regions, including the hippocampus (Papadopoulos et al., 2007, 2008). This results in decreases in GABAergic neurotransmission, deficiencies in synaptic plasticity, increased levels of anxiety, and impaired spatial learning in CB KO mice. In humans, a mutation in *ARHGEF9*, the gene that encodes CB, was first identified in a patient with epileptic encephalopathy (Harvey et al., 2004) but additional pathogenic mutations have since been identified in patients, contributing to a spectrum of ailments that include epilepsy, hyperekplexia, intellectual disability, anxiety, autism, and schizophrenia (Marco et al., 2008; Kalscheuer et al., 2009; Lesca et al.,

2011; Shimojima et al., 2011; Lionel et al., 2013; Long et al., 2015; Bhat et al., 2016; Klein et al., 2017; Wang et al., 2018; Aarabi et al., 2019; Chiou et al., 2019; Yao et al., 2020).

Overexpression of gephyrin or GABA_ARs does not significantly affect synaptic GABA_AR or gephyrin clustering in cultured hippocampal neurons (Chiou et al., 2011). However, it has been demonstrated that overexpression of CBSH3- in cultured hippocampal neurons induces the formation of large synaptic gephyrin and GABA_AR clusters (Kalscheuer et al., 2009; Chiou et al., 2011; Tyagarajan et al., 2011; Soykan et al., 2014). In the present study, we examined the effect of overexpressing a constitutively active isoform of CB, CB2SH3-, in selected cells of the dorsal hippocampus in adult mice. By overexpressing CB2SH3- in specific neuron-types, and in adulthood, we aimed to address whether the increase in CB2SH3- expression enhances the postsynaptic accumulation of gephyrin and GABA_ARs, GABAergic synaptic transmission in the developed hippocampus, and whether it can effectively protect against pentylenetetrazole (PTZ)-induced acute seizures.

Materials and Methods

Animals

All animals included in this study were treated following protocols approved by the Institutional Animal Care and Use Committee (IACUC) at the University of Connecticut and follow National Institute of Health guidelines. Both male and female mice of VGAT-IRES-Cre (JAX: Slc32a1tm2(cre)Lowl/J; stock #016962) or VGLUT1-IRES2-Cre (JAX: B6;129S-Slc17a7tm1.1(cre)Hze/J; stock #023527) background were used.

Materials

For immunofluorescence studies, mouse mAb gephyrin (1:200; RRID: https://scicrunch.org/resolver/AB_887717), guinea pig anti-VGAT (1:1000; RRID: [AB_887873](https://scicrunch.org/resolver/AB_887873)), and rabbit anti-CB (1:1000; RRID: [AB_2619977](https://scicrunch.org/resolver/AB_2619977)), were from Synaptic Systems. The rabbit anti-CB antibody detects both CBSH3- and CBSH3+ isoforms (Soykan et al., 2014; George et al., 2021). Mouse anti-HA (1:1000; RRID: [AB_10063630](https://scicrunch.org/resolver/AB_10063630)) was from Covance. The rabbit antibody against GABA_AR-subunit γ 2 (1:25; RRID: [AB_2314477](https://scicrunch.org/resolver/AB_2314477); to amino acids 1–15: QKSDDDYEDYASNKT) was raised and affinity-purified (on immobilized antigen peptide) in our laboratory. In cultured hippocampal neurons and in brain tissue, this antibody shows clustered labeling that co-localizes highly with that of antibodies to other GABA_AR subunits and to gephyrin. It also shows apposition to glutamate decarboxylase (GAD)-containing terminals. It has been described and characterized elsewhere (Khan et al., 1994; Christie and De Blas, 2003; Charych et al., 2004a,b; Li et al., 2005b, 2007, 2010, 2012; Serwanski et al., 2006; Yu et al., 2007, 2008; Chiou et al., 2011; Jin et al., 2014; Fekete et al., 2015, 2017). Species-specific anti-IgG secondary antibodies were raised in goat and labeled with Alexa Fluor 568 or 647 (Invitrogen). PTZ (catalog #18682) used for behavioral studies was from Cayman Chemicals. For

This work was supported by the National Institutes of Health National Institute of Neurological Disorders and Stroke Grant R01NS038752 (to A.L.D.) and by a University of Connecticut Research Incentive Program grant (A.L.D.).

Acknowledgements: We thank Prof. K. Harvey (UCL School of Pharmacy, London, UK) and Prof. R. J. Harvey (University of the Sunshine Coast, Sippy Downs, Australia) for providing the Myc-CB plasmid.

Correspondence should be addressed to Angel L. De Blas at angel.deblas@uconn.edu.

<https://doi.org/10.1523/ENEURO.0561-20.2021>

Copyright © 2021 George et al.

This is an open-access article distributed under the terms of the Creative Commons Attribution 4.0 International license, which permits unrestricted use, distribution and reproduction in any medium provided that the original work is properly attributed.

electrophysiological studies, tetrodotoxin (TTX; catalog #T-550) was from Alomone Labs; CNQX (catalog #C127) and picrotoxin (catalog #P1675) were from Sigma.

Construction and production of AAV9/hSyn-DIO-HA-CB2SH3(-)-IRES-mCitrine

The cDNA for the constitutively active isoform of CB tagged with HA (HA-CB2SH3-) was cloned into the pAAV2-hSyn-dF-HA-KORD-IRES-mCitrine plasmid (gift from Bryan Roth; Addgene plasmid # 65417; <http://n2t.net/addgene:65417>; RRID: https://scicrunch.org/resolver/Addgene_65417) to replace HA-KORD. The pAAV2-hSyn-DIO-HA-CB2SH3(-)-IRES-mCitrine was sent to the UNC Vector Core for AAV9 production (Zhu et al., 2014). This plasmid has been submitted to Addgene (<https://www.addgene.org/160069/>).

Viral infusion *in vivo*

Adult mice (five to eight weeks old) were anesthetized with isoflurane and placed into a stereotactic frame to prevent any head movement. The viral constructs, AAV9-hSyn-DIO-HA-CB2SH3(-)-IRES-mCitrine (HACB2-AAV) or AAV5-hSyn-DIO-EGFP (EGFP-AAV; UNC Vector Core; Roth Lab) were injected into the dorsal hippocampus (from bregma: anterior-posterior: -2.0, medial-lateral: \pm 1.6, dorsal-ventral: -1.6) using a 1- μ l Hamilton syringe at a rate of 20 nl/min, followed by 5 min before retraction of the syringe. Volumes used were 250 nl unilaterally for immunohistochemical studies and 500 nl bilaterally for electrophysiological and behavioral studies (titers: 7.2×10^{12} vg/ml EGFP-AAV; 7.1×10^{12} vg/ml HACB2-AAV). After surgery, mice were returned to their cages for two to four weeks of recovery before use for behavioral, electrophysiology, or immunohistochemical study.

Tissue preparation, immunohistology, and image acquisition

Three weeks after unilateral viral injection, mice were deeply anesthetized with an overdose of ketamine/xylazine (60/8 mg/kg) and cardiac perfusion was performed with 0.12 M phosphate buffer (PB; pH 7.4) followed by 4% PLP fixative in 0.12 M PB (4% paraformaldehyde, 1.37% lysine, and 0.21% sodium periodate). Brains were cryoprotected with 30% sucrose, frozen, and sectioned with a freezing microtome (25 μ m thick) and stored in 0.02% sodium azide in 0.1 M PB, pH 7.4 at 4°C. Immunofluorescence was performed as described elsewhere (Li et al., 2005a; Fekete et al., 2017; Miralles et al., 2020). Briefly, free-floating brain sections were incubated with 5% normal goat serum, 0.3% Triton X-100 in 0.1 M PB for 1 h at room temperature. Sections were then incubated for 2 d in primary antibody cocktails raised in different species in 2% NGS/0.3% Triton X-100 in 0.1 M PB at 4°C. Sections were washed and incubated in a mixture of fluorophore-conjugated secondary antibodies in 2% NGS/0.3% Triton X-100 in 0.1 M PB for 1 h at room temperature. When necessary, a DAPI counterstain (200 nm) was applied following a wash after secondary incubation. Sections were then washed again and mounted onto gelatin-coated glass slides with Prolong Gold Antifade

mounting solution (Invitrogen). Confocal images of brain sections were acquired using an A1R laser scanning confocal microscope (Nikon Instruments) with a Plan Apo VC 60 \times /1.4 oil immersion objective. For the quantifications presented in Figure 1. The images were collected with a LSM 800 confocal laser-scanning microscope (Zeiss) with a 63 \times /1.4 oil-immersion objective. The pinhole was set at 1.2 Airy units. Images were collected as single optical sections. The low-magnification images of brain sections for EGFP/mCitrine/DAPI were collected by epifluorescence with a Plan Fluor 10 \times /0.3 objective.

Electrophysiological recordings

Mice were anesthetized by administration of ketamine (375 mg/kg, i.p.) and xylazine (25 mg/kg, i.p.) and rapidly decapitated; cortex was removed, and slices (250 μ m) were cut using a microslicer (DSK 1500E; Dosaka) in ice-cold substituted Ringer solution containing the following: 83 mM NaCl, 26 mM NaHCO₃, 1.25 mM NaH₂PO₄, 2.5 mM KCl, 22 mM dextrose, 72 mM sucrose, 0.5 mM MgCl₂, 3.3 mM CaCl₂, 1.3 mM Na-ascorbate, and 0.6 mM Na-pyruvate. Slices were incubated for 30 min at 37°C and kept at room temperature in a normal Ringer's solution containing: 140 mM NaCl, 3 mM KCl, 2 mM MgCl₂, 2 mM CaCl₂, 10 mM HEPES, and 10 mM glucose. Both substituted and normal Ringer's solutions were bubbled with 95% O₂ and 5% CO₂ (pH 7.3).

Individual slices containing the CA1 hippocampus were transferred to a recording chamber mounted on a fixed-stage microscope (Olympus BX5.1WI) and perfused continuously (~2 ml/min) with normal Ringer's solution (equilibrated with 5% CO₂; pH 7.3). Transfected CA1 hippocampal neurons were visually identified by fluorescent signal from EGFP or mCitrine. All recordings were made with an Axopatch 200B patchclamp amplifier, digitized with a Digidata 1322A A/D converter, and recorded using pCLAMP 10.0 software (Molecular Devices). Recordings were obtained at room temperature (~22°C) with patch electrodes pulled from borosilicate glass capillaries (Harvard Apparatus) on a two-stage puller (P-97; Sutter Instrument) to a DC resistance of 5–7 M Ω when filled with a pipette solution containing the following: 130 mM CsCl, 8.5 mM NaCl, 5 mM HEPES, 4 mM MgCl₂, 4 mM Mg²⁺-ATP, 0.3 mM Na-GTP, and 0.6 mM EGTA. Electrode tips were coated with Sylgard 184 (Dow Corning). A gigaohm seal (\geq 1 G Ω) was achieved using a cell-attached voltage-clamp configuration with holding potential matched to the resting membrane potential ($V_{\text{hold}} = -70$ mV) and with no current generated by the amplifier ($I_{\text{amp}} = 0$ pA). Whole-cell access (\leq 20 M Ω) was obtained to characterize spontaneous synaptic input. Spontaneous mIPSCs were characterized in the presence of bath applied CNQX (10 μ M) and TTX (0.5 μ M), and events were confirmed with bath application of picrotoxin (100 μ M). mIPSCs were analyzed using Clampfit 10.7 and detected with characteristic kinetics (fast rising phase followed by a slow decay). Each automatically detected event was also visually inspected to exclude false positives. Recordings were discarded if Ra varied 10%

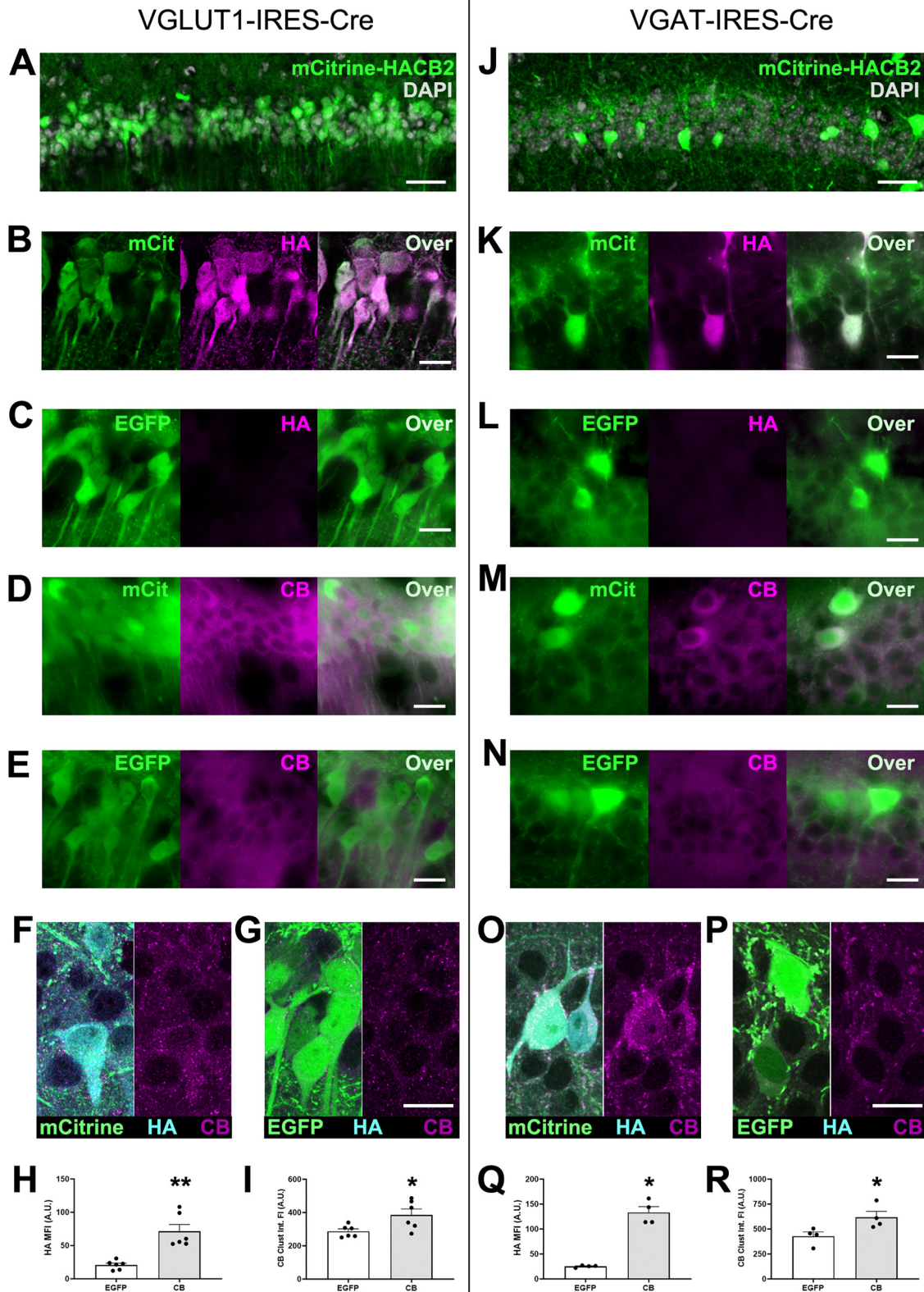


Figure 1. Injection of hippocampal CA1 with AAV-DIO-HA-CB2SH3(-)-IRES-mCitrine results in overexpression of mCitrine and HA-CB2SH3 (-) in a cre-dependent manner. **A–I**, The mCitrine-HACB2-AAV (**A**, **B**, **D**, **F**) or a control EGFP-AAV (**C**, **E**, **G**) were injected into CA1 of VGLUT1-IRES-cre mice, resulting in expression of mCitrine or EGFP in the glutamatergic pyramidal cell, and images were taken with epifluorescence microscopy (**A–E**) or confocal microscopy (**F**, **G**). In mCitrine-HACB2-AAV-injected mice, the transduced pyramidal cells expressing

continued

mCitrine also overexpressed HA-CB2SH3⁻, as detected by Ms anti-HA (**B, F**) and Rb anti-CB (**D, F**). In CA1 of EGFP-AAV-injected mice, HA was not detected (**C, G**), and only a low endogenous level of CB (**E, G**) was visible. Quantification from confocal images for mean intensity of HA immunofluorescence in SP is presented in **H**, and integrated intensity of CB immunofluorescent clusters is presented in **I**. **J–R**, The mCitrine-HACB2-AAV (**J, K, M, O**) or a control EGFP-AAV (**L, N, P**) were injected into CA1 of VGAT-IRES-cre mice, resulting in overexpression of mCitrine or EGFP in GABAergic interneurons and images were taken with epifluorescence microscopy (**J–N**) or confocal microscopy (**O–P**). In mCitrine-HACB2-AAV-injected mice, the transduced interneurons expressed mCitrine and overexpressed HA-CB2SH3⁻, as detected by Ms anti-HA (**K, O**) and Rb anti-CB (**M, O**). In CA1 of EGFP-AAV-injected mice, HA was not detected (**L, P**), and only a low endogenous level of CB (**N, P**) was visible. Quantification from confocal images for mean intensity of HA immunofluorescence in interneurons is presented in **Q**, and integrated intensity of perisomatic CB immunofluorescent clusters is presented in **R**. Scale bars: 25 μm (**A, J**) and 10 μm (**B–G, K–P**). Asterisks in the quantification graphs indicate significance using Mann-Whitney U test, * $p < 0.05$, ** $p < 0.01$.

during an experiment, and capacitance and Ra compensation (70%) were used to minimize voltage errors.

Behavioral study

Preliminary trials were performed on naive mice to determine dose of PTZ that would reliably induce acute seizures while minimizing mortality. Three weeks after bilateral viral infusion, mice were subjected to behavioral study. Mice were given a single injection of PTZ (40 mg/kg, i.p.) to induce acute seizures. The mice were then placed into a cage and behavior was observed. Seizures were scored according to a modified Racine scale (Racine, 1972; Lüttjohann et al., 2009; Singh et al., 2016) with the following scores: 1, sudden behavioral arrest; 2, facial jerking; 3, myoclonic jerks; 4, clonic seizure, sitting; 5, clonic, tonic-clonic seizure, lying on belly; 6, clonic, tonic-clonic seizure with loss of posture and wild jumping; with notation of time of onset of each intensity of seizure and tallying of maximal seizure intensity in 2-min bins. Seizure behavior typically subsides by 30 min after PTZ administration, so animals were then returned to their home cages. Animals were killed, brains collected, and sections examined by epifluorescence microscopy to confirm appropriate transduction of hippocampal CA1.

Experimental design and statistical analysis

All image analysis was performed using ImageJ (RRID: SCR_003070). For analysis of immunofluorescence, brain sections were analyzed from mice injected with HACB2-AAV (VGLUT1-cre: $n = 6$, VGAT-cre: $n = 4$) or EGFP-AAV (VGLUT1-cre: $n = 6$, VGAT-cre: $n = 4$). For each animal, each quantified value is the average of 10–15 measurements [regions of interest (ROIs) or individual interneurons], as explained below. Because of the densely packed nature of transduced CA1 pyramidal cells in VGLUT1-cre mice, ROIs were used to measure impact of viral transduction. In each section, five images were taken per hemisphere, and three ROIs with areas of 500 μm^2 were created within stratum pyramidale (SP) of CA1 in each to determine changes in perisomatic synapses. These values were averaged to present a single value for each animal. This was repeated within stratum radiatum (SR) and stratum oriens (SO) to measure changes in dendritic synapses. To determine changes in synaptic proteins in transduced interneurons of CA1 (of VGAT-cre mice), cell bodies within SP were outlined and then expanded inward/outward to create a 15-pixel thick ring-shaped ROI around transduced neurons. VGAT, gephyrin, and

GABA_AR- $\gamma 2$ -subunit immunoreactivities were then measured in these ROIs. Five to seven cells were measured per brain section, two sections per animal, to calculate an average value for each animal. Since only one hemisphere was injected, the other hemisphere served as an internal control to ensure there was no significant variability from mouse to mouse. Additional injected mice were excluded from study in cases of off-target injection or lack of transduction (VGAT-cre: four mice, VGLUT1-cre: three mice). For electrophysiological and behavioral study in VGLUT1-cre mice, mice were injected bilaterally. For electrophysiological experiments, data are presented from transduced cells (HACB2-AAV: $n = 5$, EGFP-AAV: $n = 6$; 1 cell per mouse) from injected mice. The final 100 events before bath application of picrotoxin was used for analysis. For behavioral experiments, data are presented for injected mice (HACB2-AAV: $n = 15$, EGFP-AAV: $n = 12$), and the observer was blinded to the condition of the mouse during seizure scoring. Additional injected mice were excluded from study if they died after PTZ administration (HACB2-AAV: one mouse, EGFP-AAV: two mice) or if brain examination determined off-target injection or lack of transduction. No additional mortality was observed during or following procedures in adeno-associated virus (AAV)-injected mice. Statistical analyses were performed using Prism 8 (GraphPad). Statistical tests include Mann-Whitney U tests for two-group comparisons when sample size was below 10, and unpaired t tests when sample size was > 10 , Kolmogorov–Smirnov tests, and Fisher's exact test. Statistical data can be found in Table 1. Summary data are presented as mean \pm SEM from n mice or neurons, as indicated.

Results

Mice injected with AAV-HA-CB2SH3⁻ express both mCitrine and HA-CB

In order to validate that our cre-dependent viral construct was capable of transduction of appropriate cells in CA1, we examined the pattern of mCitrine and HA expression in injected mice.

In VGLUT1-IRES-cre mice injected with the HACB2-AAV, large swathes of the pyramidal cell layer in CA1 expressed mCitrine (Fig. 1A), interspersed with the occasional non-transduced cell, likely indicating an interneuron. As expected, none of the cells in SO were transduced, since cell bodies there belong to GABAergic cells. The transduced cells showing mCitrine fluorescence also

Table 1: Descriptive and summary statistics by figure

Data	Figure	Statistical test	Test values	<i>p</i> value
Immunofluorescence data:				
<i>VGLUT1-cre</i> :				
HA MFI	1	Mann–Whitney <i>U</i> test	Median EGFP: 22.09 Median CB: 57.90 <i>N</i> = 6, <i>U</i> = 0	0.0022
CB integrated FI	1	Mann–Whitney <i>U</i> test	Median EGFP: 283.3 Median CB: 384.7 <i>N</i> = 6, <i>U</i> = 5	0.0411
SO Geph size	2	Mann–Whitney <i>U</i> test	Median EGFP: 0.2559 Median CB: 0.3428 <i>N</i> = 6, <i>U</i> = 0	0.0022
SP Geph size	2	Mann–Whitney <i>U</i> test	Median EGFP: 0.1923 Median CB: 0.2491 <i>N</i> = 6, <i>U</i> = 2	0.0087
SR Geph size	2	Mann–Whitney <i>U</i> test	Median EGFP: 0.2360 Median CB: 0.2838 <i>N</i> = 6, <i>U</i> = 4	0.0260
SO Geph density	2	Mann–Whitney <i>U</i> test	Median EGFP: 0.1133 Median CB: 0.1691 <i>N</i> = 6, <i>U</i> = 1	0.0043
SP Geph density	2	Mann–Whitney <i>U</i> test	Median EGFP: 0.0723 Median CB: 0.1331 <i>N</i> = 6, <i>U</i> = 3	0.0152
SR Geph density	2	Mann–Whitney <i>U</i> test	Median EGFP: 0.1136 Median CB: 0.1922 <i>N</i> = 6, <i>U</i> = 3	0.0152
SO γ 2 size	2	Mann–Whitney <i>U</i> test	Median EGFP: 0.1760 Median CB: 0.1715 <i>N</i> = 6, <i>U</i> = 11	0.8413
SP γ 2 size	2	Mann–Whitney <i>U</i> test	Median EGFP: 0.1647 Median CB: 0.2013 <i>N</i> = 6, <i>U</i> = 2	0.0317
SR γ 2 size	2	Mann–Whitney <i>U</i> test	Median EGFP: 0.1522 Median CB: 0.1562 <i>N</i> = 6, <i>U</i> = 10	0.6905
SO γ 2 density	2	Mann–Whitney <i>U</i> test	Median EGFP: 0.0879 Median CB: 0.0975 <i>N</i> = 6, <i>U</i> = 12	>0.9999
SP γ 2 density	2	Mann–Whitney <i>U</i> test	Median EGFP: 0.0865 Median CB: 0.0824 <i>N</i> = 6, <i>U</i> = 12	>0.9999
SR γ 2 density	2	Mann–Whitney <i>U</i> test	Median EGFP: 0.0615 Median CB: 0.0877 <i>N</i> = 6, <i>U</i> = 6	0.2222
SO VGAT size	2	Mann–Whitney <i>U</i> test	Median EGFP: 0.2082 Median CB: 0.2406 <i>N</i> = 6, <i>U</i> = 9	0.1797
SP VGAT size	2	Mann–Whitney <i>U</i> test	Median EGFP: 0.2447 Median CB: 0.2910 <i>N</i> = 6, <i>U</i> = 10	0.2403
SR VGAT size	2	Mann–Whitney <i>U</i> test	Median EGFP: 0.2015 Median CB: 0.2072 <i>N</i> = 6, <i>U</i> = 12	0.3939
SO VGAT density	2	Mann–Whitney <i>U</i> test	Median EGFP: 0.0594 Median CB: 0.0716 <i>N</i> = 6, <i>U</i> = 10	0.2229
SP VGAT density	2	Mann–Whitney <i>U</i> test	Median EGFP: 0.0705 Median CB: 0.0799 <i>N</i> = 6, <i>U</i> = 7	0.0931
SR VGAT density	2	Mann–Whitney <i>U</i> test	Median EGFP: 0.0778 Median CB: 0.0787 <i>N</i> = 6, <i>U</i> = 16	0.8182

(Continued)

Table 1: Continued

Data	Figure	Statistical test	Test values	<i>p</i> value
VGAT-cre				
HA MFI	1	Mann–Whitney <i>U</i> test	Median EGFP: 25.93 Median CB: 128.9 <i>N</i> = 4, <i>U</i> = 0	0.0286
CB integrated FI	1	Mann–Whitney <i>U</i> test	Median EGFP: 450.8 Median CB: 580.9 <i>N</i> = 4, <i>U</i> = 0	0.0286
Geph size	3	Mann–Whitney <i>U</i> test	Median EGFP: 0.1788 Median CB: 0.3437 <i>N</i> = 4, <i>U</i> = 0	0.0286
Geph density	3	Mann–Whitney <i>U</i> test	Median EGFP: 0.2291 Median CB: 0.4403 <i>N</i> = 4, <i>U</i> = 0	0.0286
γ 2 size	3	Mann–Whitney <i>U</i> test	Median EGFP: 0.1706 Median CB: 0.2151 <i>N</i> = 4, <i>U</i> = 1	0.0571
γ 2 density	3	Mann–Whitney <i>U</i> test	Median EGFP: 0.1387 Median CB: 0.1386 <i>N</i> = 4, <i>U</i> = 8	>0.9999
VGAT size	3	Mann–Whitney <i>U</i> test	Median EGFP: 0.3144 Median CB: 0.3617 <i>N</i> = 4, <i>U</i> = 4	0.3429
VGAT density	3	Mann–Whitney <i>U</i> test	Median EGFP: 0.2008 Median CB: 0.2967 <i>N</i> = 4, <i>U</i> = 5	0.4857
Electrophysiology data				
mIPSC amplitude cumulative frequency	4	Kolmogorov–Smirnov test	Kolmogorov–Smirnov <i>D</i> = 0.3283 <i>N</i> = 600, 500	<0.0001
mIPSC amplitude	4	Mann–Whitney <i>U</i> test	Median EGFP: –29.84 Median CB: –41.98 <i>N</i> = 6, 5, <i>U</i> = 4	0.0455
mIPSC frequency cumulative frequency	4	Kolmogorov–Smirnov test	Kolmogorov–Smirnov <i>D</i> = 0.1651 <i>N</i> = 600, 500	<0.0001
mIPSC frequency	4	Mann–Whitney <i>U</i> test	Median EGFP: 0.2125 Median CB: 0.4583 <i>N</i> = 6, 5, <i>U</i> = 0	0.0043
mIPSC rise time	4	Mann–Whitney <i>U</i> test	Median EGFP: 0.9404 Median CB: 1.127 <i>N</i> = 6, 5, <i>U</i> = 0	0.0043
mIPSC decay Tau	4	Mann–Whitney <i>U</i> test	Median EGFP: 15.22 Median CB: 18.40 <i>N</i> = 6, 5, <i>U</i> = 6	0.1255
Behavioral data				
Cumulative seizure score	5	Kolmogorov–Smirnov test	Kolmogorov–Smirnov <i>D</i> = 0.7333 <i>N</i> = 12, 15	0.0006
Latency to seizure score 1	5	Unpaired <i>t</i> test	Mean EGFP: 76.42 Mean CB: 216.1 <i>N</i> = 12, 14, <i>F</i> = 55.84, <i>DF</i> _n = 13, <i>Dfd</i> = 11	0.0358
Latency to seizure score 2	5	Unpaired <i>t</i> test	Mean EGFP: 83.33 Mean CB: 260.0 <i>N</i> = 12, 14, <i>F</i> = 90.32, <i>DF</i> _n = 13, <i>Dfd</i> = 11	0.0480
Latency to seizure score 3	5	Unpaired <i>t</i> test	Mean EGFP: 108.4 Mean CB: 252.5 <i>N</i> = 12, 11, <i>F</i> = 45.64, <i>DF</i> _n = 10, <i>Dfd</i> = 11	0.0912
Latency to seizure score 4	5	Unpaired <i>t</i> test	Mean EGFP: 167.6 Mean CB: 269.9 <i>N</i> = 12, 9, <i>F</i> = 5.961, <i>DF</i> _n = 8, <i>Dfd</i> = 11	0.1815
Latency to seizure score 5	5	Unpaired <i>t</i> test	Mean EGFP: 210.5 Mean CB: 381.0 <i>N</i> = 10, 5, <i>F</i> = 10.95, <i>DF</i> _n = 4, <i>Dfd</i> = 9	0.1062

(Continued)

Table 1: Continued

Data	Figure	Statistical test	Test values	<i>p</i> value
Latency to seizure score 6	5	Unpaired <i>t</i> test	Mean EGFP: 239.9 Mean CB: 298.0	0.5353
Contingency seizure score 1	5	Fisher's exact test	$N=9, 2, F=n/a, DFn=n/a, Dfd=n/a$ EGFP: 12, 0 CB: 14, 1 Total: 26, 1 (seized, did not)	>0.9999
Contingency Seizure score 2	5	Fisher's exact test	EGFP: 12, 0 CB: 14, 1 Total: 26, 1 (seized, did not)	>0.9999
Contingency seizure score 3	5	Fisher's exact test	EGFP: 12, 0 CB: 11, 4 Total: 23, 4 (seized, did not)	0.1060
Contingency seizure score 4	5	Fisher's exact test	EGFP: 12, 0 CB: 9, 6 Total: 21, 6 (seized, did not)	0.0200
Contingency seizure score 5	5	Fisher's exact test	EGFP: 10, 5 CB: 5, 10 Total: 15, 12 (seized, did not)	0.0185
Contingency seizure score 6	5	Fisher's exact test	EGFP: 9, 3 CB: 2, 13 Total: 11, 16 (seized, did not)	0.0020

expressed HA-CB2SH3⁻, as detected by immunoreactivity with Ms anti-HA (Fig. 1B) and increased immunoreactivity with Rb anti-CB (Fig. 1D). In CA1 of the VGLUT1-IRES-cre mice injected with the EGFP-AAV, we did not detect any HA (Fig. 1C), nor any increased levels of CB (Fig. 1E). To quantify the extent to which CB was expressed over endogenous levels, confocal images were taken (Fig. 1F,G). Mean immunofluorescence intensity (MFI) of HA was significantly increased in HACB2-AAV-transduced neurons (CB: 71.4 ± 10.3 A.U.; EGFP: 20.8 ± 2.8 A.U.; Mann-Whitney *U* test, $p=0.002$; Fig. 1H). Immunofluorescence with the rabbit anti-CB antibody showed that while there was no significant change in the size of CB clusters (Mann-Whitney *U* test, $p=0.49$), there were increases in the density (CB: 0.265 ± 0.017 clusters/ μm^2 ; EGFP: 0.227 ± 0.021 clusters/ μm^2 ; Mann-Whitney *U* test, $p=0.041$) and integrated fluorescence intensity of the immunopositive puncta (CB: 386.2 ± 35.4 A.U.; EGFP: 287.4 ± 14.6 A.U.; Mann-Whitney *U* test, $p=0.041$; Fig. 1I).

In injected VGAT-IRES-cre mice, mCitrine expression in dorsal hippocampal CA1 matched the expected distribution of interneurons (Fig. 1J), with transduced cells scattered through pyramidal cell layer, as well as cell bodies in the SO. Since our viral construct was inducing bicistronic expression of mCitrine and HA-CB2SH3⁻, we confirmed that transduced cells were also expressing HA-CB2SH3⁻. We were able to detect both HA (Fig. 1K) and an increased level of CB (Fig. 1M) in transduced cells of CA1 in mice injected with the HACB2-AAV compared with EGFP-AAV-injected mice (Fig. 1L,N, respectively). As expected, all neurons in the SP of EGFP-AAV-injected mice showed endogenous CB expression. However, in HACB2-AAV transduced interneurons, CB expression was noticeably stronger than the endogenous CB expression of either the surrounding non-transduced pyramidal neurons (Fig. 1M) or interneurons transduced with EGFP-AAV (Fig. 1M vs N, O vs P). Analysis of confocal images (Fig. 1O,P) revealed

that HA MFI is significantly increased in HACB2-AAV transduced interneurons (CB: 133.3 ± 11.7 A.U.; EGFP: 25.3 ± 1.1 A.U.; Mann-Whitney *U* test, $p=0.029$; Fig. 1Q) as is integrated fluorescence intensity of CB puncta (CB: 617.6 ± 59.5 ; EGFP: 428.3 ± 42.6 A.U.; Mann-Whitney *U* test, $p=0.029$; Fig. 1R). While there was no change in the density of the clusters (Mann-Whitney *U* test, $p=0.69$), there was a moderate but not significant increase in size of clusters (CB: 0.211 ± 0.019 μm^2 ; EGFP: 0.161 ± 0.008 μm^2 Mann-Whitney *U* test, $p=0.057$).

Conditional overexpression of HA-CB2SH3⁻ in CA1 pyramidal neurons results in enhanced gephyrin and perisomatic GABAAR- $\gamma 2$ clusters in VGLUT1-cre mice

To investigate the extent to which overexpression of HA-CB2SH3⁻ affects hippocampal GABAergic synapses, we examined presynaptic and postsynaptic protein expression in HACB2-AAV transduced glutamatergic pyramidal cells of CA1 (Fig. 2A), as compared with those transduced with EGFP-AAV (Fig. 2B). Because of the packed nature of the transduced hippocampal pyramidal cells, regions within CA1 were examined rather than individual transduced cells: ROIs within the SP that contain the cell bodies of the pyramidal cells, or ROIs within SO or SR populated by processes of the pyramidal cells. In VGLUT1-cre mice injected with the HACB2-AAV, there were significant increases in average size of gephyrin clusters in each region of the transduced CA1 (SO: CB: 0.343 ± 0.015 μm^2 , EGFP: 0.253 ± 0.008 μm^2 ; SP: CB: 0.247 ± 0.011 μm^2 , EGFP: 0.195 ± 0.008 μm^2 ; SR: CB: 0.288 ± 0.014 μm^2 , EGFP: 0.229 ± 0.008 μm^2 ; Mann-Whitney *U* test, $p=0.002$, $p=0.009$, $p=0.026$; respectively; Fig. 2C). The gephyrin clusters in these regions of HACB2-AAV-transduced CA1 also had increased MFI in the SO (32.4% increase), SP (61.5% increase), and SR (43.7% increase) compared with EGFP-AAV-transduced

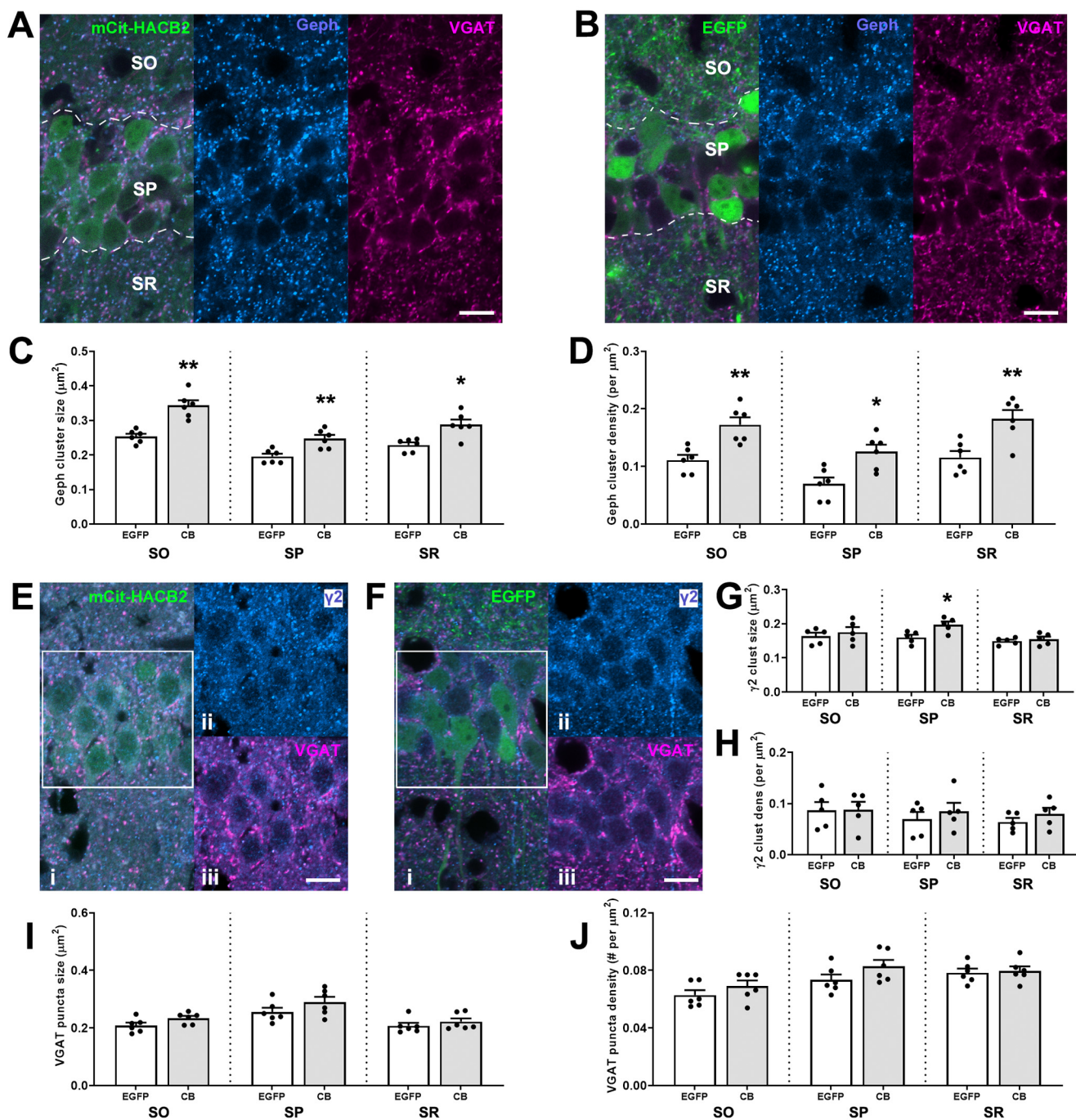


Figure 2. Overexpression of HA-CB2SH3– in hippocampal CA1 pyramidal cells of the VGLUT1-IRES-cre mouse results in larger postsynaptic gephyrin clusters without observed alteration of the presynaptic GABAergic input. **A, B**, Representative IF images of CA1 pyramidal cells transduced with mCitricine-HACB2-AAV (**A**) or EGFP-AAV (**B**) labeled with Ms anti-Geph (blue) and GP anti-VGAT (magenta). Outlined in **A, B** are rough borders for SO, SP, and SR. **C, D**, Quantification of size (**C**) and density (**D**) of gephyrin clusters in these regions. **E, F**, Representative IF images of CA1 pyramidal cells transduced with mCitricine-HACB2-AAV (**E**) or EGFP-AAV (**F**) labeled with Ms anti- $\gamma 2$ (blue; **i, ii**) and GP anti-VGAT (magenta; **i, iii**). Panels **ii, iii** show individual channels for blue and red for SP as outlined in the box in **i**. **G, H**, Quantification of size (**G**) and density (**H**) of GABA_A $\gamma 2$ clusters in these regions. **I, J**, Quantification of size (**I**) and density (**J**) of VGAT puncta in these regions. Each dot represents the mean for quantification for one animal, and error bars indicate SEM. At least two sections were processed per animal, with three ROIs in each region (SO, SP, SR) for each of five images for each hemisphere (total sampled area per region/hemisphere = 7500 μm^2). Scale bar: 10 μm . Asterisks in the quantification graphs indicate significance using Mann–Whitney *U* test; **p* < 0.05, ***p* < 0.01.

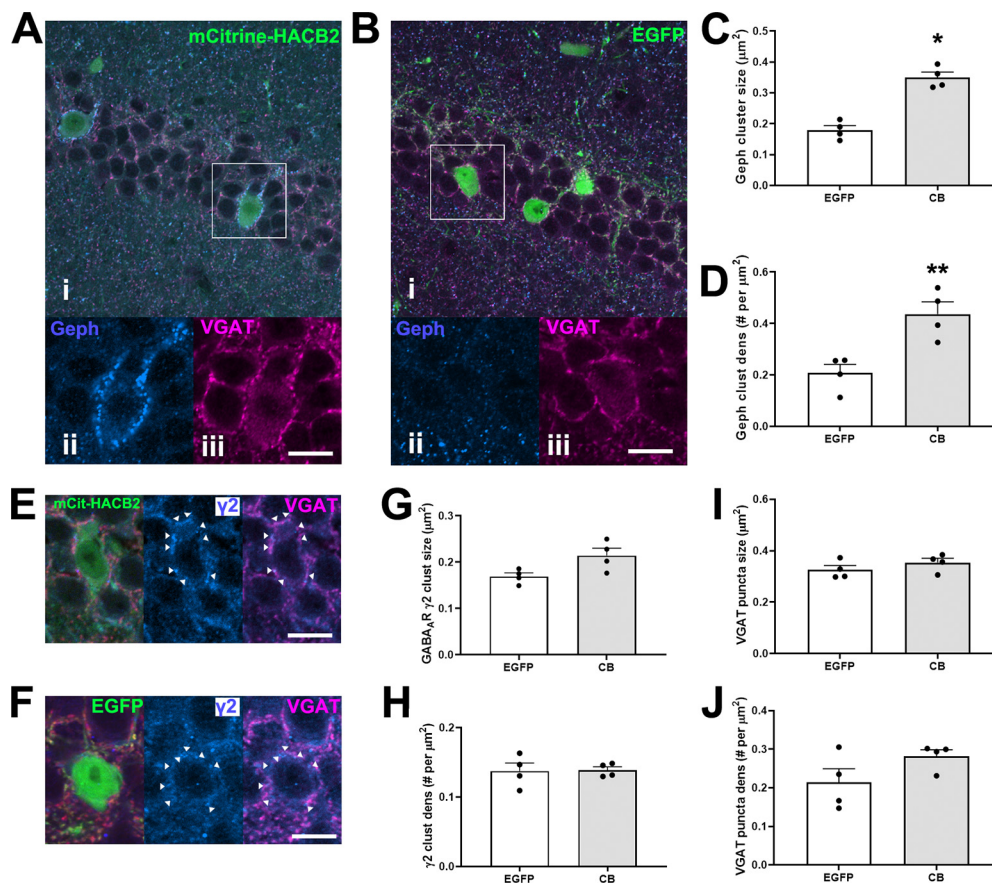


Figure 3. Overexpression of HA-CB2SH3⁻ in hippocampal interneurons of the VGAT-IRES-cre mouse results in larger gephyrin clusters without observed alterations of presynaptic VGAT input. **A, B**, Representative IF images of CA1 interneurons transduced with mCitrine-HACB2-AAV (**A**) or EGFP-AAV (**B**) labeled with Ms anti-Geph (blue; **ii**) and GP anti-VGAT (magenta; **iii**). Inset of boxes in **i** are shown in **ii, iii**. **C, D**, Quantification of the size (**C**) and density (**D**) of the gephyrin clusters on the perimeter of the transduced cells. **E, F**, Representative IF images of CA1 interneurons transduced with mCitrine-HACB2-AAV (**E**) or EGFP-AAV (**F**) labeled with Rb anti-γ2 (blue; **ii**) and GP anti-VGAT (magenta; **iii**). **G, H**, The size (**G**) and density (**H**) of the GABA_A γ2 clusters on the perimeter of the transduced cells were quantified. The size (**I**) and density (**J**) of the VGAT puncta surrounding the transduced cell have been quantified. Each dot represents one animal and error bars indicate SEM. Two sections per animal were processed and at least five cells per brain section were quantified. Scale bars: 20 μm (**A, Bi**) and 10 μm (**A, Bii, Biii, E, F**). Asterisks in the quantification graphs indicate significance using Mann–Whitney *U* test; **p* < 0.05, ***p* < 0.01.

CA1 (Mann–Whitney *U* test, *p* = 0.026, *p* = 0.004, and *p* = 0.009, respectively). There were also more clusters in these regions of transduced CA1 (SO: CB: 0.172 ± 0.013 per μm², EGFP: 0.111 ± 0.009 per μm²; SP: CB: 0.126 ± 0.012 per μm², EGFP: 0.070 ± 0.11 per μm²; SR: CB: 0.183 ± 0.015 per μm², EGFP: 0.116 ± 0.011 per μm²; Mann–Whitney *U* test, *p* = 0.004, *p* = 0.015, and *p* = 0.015; respectively; Fig. 2D). Size, density and MFI of gephyrin clusters were also increased compared with non-transduced contralateral hemisphere in the HACB2-AAV-injected mouse brains. There were no significant differences in any of the measured parameters between contralateral hemispheres of HACB2-AAV-injected mice and EGFP-AAV-injected mice.

In the SP of the HACB2-AAV-injected mice, there was also an increase of size of γ2 GABA_AR subunit clusters compared with the EGFP-AAV-injected mice (CB: 0.197 ± 0.009 μm² vs EGFP: 0.160 ± 0.008 μm²; Mann–Whitney *U* test, *p* = 0.032; Fig. 2E–H). No

significant differences in GABA_A γ2 density or MFI were detected in the SP. Moreover, no difference in cluster size, density or MFI were found in the SO or SR of HACB2-AAV versus EGFP-AAV-injected mice.

Regarding presynaptic VGAT expression, there was no significant change to puncta size, density, or MFI of the presynaptic VGAT in SO, SP or SR in the HACB2-AAV versus EGFP-AAV-injected mice (Fig. 2I, J).

Conditional overexpression of HA-CB2SH3⁻ enhances gephyrin clusters in CA1 interneurons in VGAT-cre mice

We examined the changes to presynaptic and postsynaptic proteins at the GABAergic synapse as a result of overexpression of HA-CB2SH3⁻ in CA1 interneurons (Fig. 3A). There was a marked increase in the size of perisomatic gephyrin clusters on neurons transduced with the HACB2-AAV (0.350 ± 0.017 μm²) compared with those transduced with the EGFP-AAV (0.179 ±

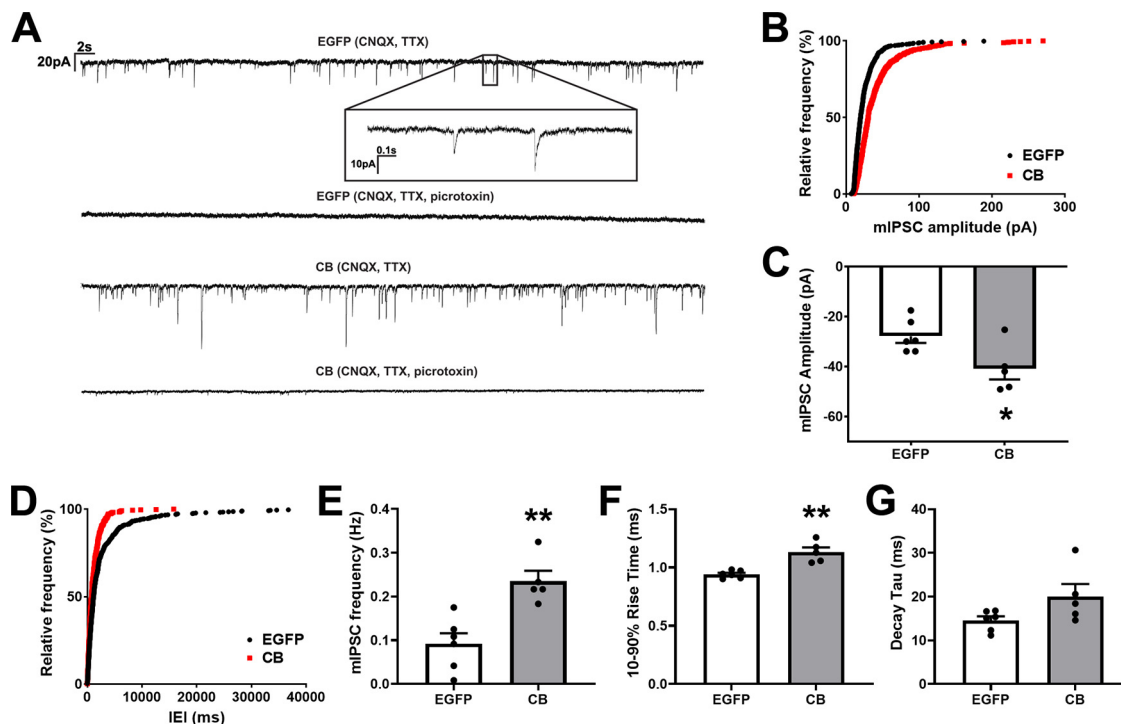


Figure 4. Pyramidal CA1 cells of the VGLUT1-IRES-cre mouse transduced with HACB2-AAV have increased strength of synaptic inhibitory neurotransmission. **A**, Representative traces showing mIPSCs from EGFP-AAV-transduced cells (top) or mCitrine-HACB2-AAV-transduced cells (bottom) that were eliminated in the presence of picrotoxin (lower trace for each). Inset of upper trace shows stereotypical mIPSCs. Vertical scale bar indicates 20 pA and horizontal bar indicates 2 s. Inset, Vertical scale bar indicates 10 pA; while horizontal bar indicates 0.1 s. **B**, Amplitudes of mIPSCs were quantified and the cumulative relative frequency displayed. **C**, The average amplitudes of mIPSCs. **D**, Interevent interval (IEI) of mIPSCs were quantified and the cumulative relative frequency displayed. **E**, Quantification of the average frequency of mIPSCs. **F**, **G**, Quantification of the average 10–90% rise time (**F**), and decay tau (**G**). For **C**, **E–G**, each dot represents one cell from which 100 events were quantified, and error bars indicate SEM. For **B**, **D**, Kolmogorov–Smirnov tests were performed; $p < 0.001$. Asterisks indicate significance using Mann–Whitney U test; $*p < 0.05$, $**p < 0.01$.

$0.015 \mu\text{m}^2$; Mann–Whitney U test, $p = 0.029$; Fig. 3A–C) and a 140% increase in MFI of clusters (Mann–Whitney U test, $p = 0.029$). This was accompanied by an increase in the density of gephyrin clusters in neurons transduced with HACB2-AAV compared with EGFP-AAV (0.436 ± 0.047 and 0.207 ± 0.034 clusters/ μm^2 , respectively; Mann–Whitney U test, $p = 0.029$; Fig. 3D). Despite gephyrin clusters in HACB2-AAV transduced interneurons being nearly twice the size, and twice as numerous as in EGFP-AAV transduced interneurons, there was only a modest, but not significant, increase in the size of GABA_AR $\gamma 2$ clusters (CB: 0.214 ± 0.016 vs EGFP: $0.169 \pm 0.008 \mu\text{m}^2$; Mann–Whitney U test, $p = 0.057$; Fig. 3E–G) and no significant change in density of clusters (CB: 0.139 ± 0.005 vs EGFP: 0.138 ± 0.011 puncta/ μm^2 ; Mann–Whitney U test, $p > 0.99$; Fig. 3H).

There were no corresponding changes in either size (CB: $0.353 \pm 0.017 \mu\text{m}^2$; EGFP: $0.325 \pm 0.017 \mu\text{m}^2$; Mann–Whitney U test, $p = 0.34$; Fig. 3I) or density (CB: 0.282 ± 0.017 puncta/ μm^2 ; EGFP: 0.214 ± 0.036 puncta/ μm^2 ; Mann–Whitney U test, $p = 0.49$; Fig. 3J) in VGAT-positive terminals synapsing onto transduced cells. Additionally, there were no differences in overall gephyrin, GABA_AR $\gamma 2$, or VGAT cluster size or density in the

contralateral CA1 between HACB2-AAV-injected and EGFP-AAV-injected mice.

Synaptic inhibitory neurotransmission is strengthened in HA-CB2SH3–overexpressing CA1 pyramidal neurons

To determine whether the enlarged gephyrin and GABA_AR clusters in VGLUT1-cre mice transduced with HACB2-AAV corresponded to stronger synaptic inhibitory neurotransmission, we measured spontaneous mIPSCs in transduced CA1 pyramidal neurons in brain slices from mice bilaterally injected with either HACB2-AAV or control EGFP-AAV. We found that in HACB2-AAV transduced CA1 pyramidal cells, there were more inhibitory events, many with higher amplitudes than in the control EGFP-AAV-transduced cells (Fig. 4A). These mIPSCs were eliminated in the presence of picrotoxin, ascertaining that they correspond to GABA_AR currents.

A cumulative relative frequency plot indicates a right shift in the amplitudes of mIPSCs in HACB2-AAV-transduced neurons (Kolmogorov–Smirnov $p < 0.001$; Fig. 4B) and greater amplitudes (CB: -40.91 ± 4.28 pA; EGFP: -27.88 ± 2.71 pA; Mann–Whitney U test, $p = 0.046$; Fig. 4C), suggesting an increase in the number of postsynaptic GABA_ARs.

The mIPSCs in HACB2-AAV-transduced cells shifted to lower interevent intervals (Kolmogorov–Smirnov, $p < 0.001$; Fig. 4D) and these transduced neurons demonstrated higher frequencies (CB: 0.537 ± 0.095 Hz; EGFP: 0.181 ± 0.036 Hz; Mann–Whitney U test, $p = 0.004$; Fig. 4E) than control EGFP-AAV cells. This finding when taken together with our results demonstrating no change in size or density of presynaptic VGAT, likely indicates a higher probability of release from presynaptic GABAergic terminals. Finally, we analyzed the rise time and decay tau of mIPSCs, to determine whether there might be any changes in receptor kinetics which might speak to alterations in distribution of receptors or receptor subunit composition. We found that while there was a significant increase in 10–90% rise times of mIPSCs in HACB2-AAV neurons (CB: 1.132 ± 0.040 ms; EGFP: 0.941 ± 0.013 ms; Mann–Whitney U test, $p = 0.004$; Fig. 4F), the increase in decay tau was not significant (CB: 20.05 ± 2.84 ms; EGFP: 14.55 ± 0.95 ms; Mann–Whitney U test, $p = 0.126$; Fig. 4G).

VGLUT1-cre mice injected with HACB2-AAV are less susceptible to acute seizures

To determine whether increased GABAergic inhibitory synaptic neurotransmission in CA1 pyramidal cells, seen in VGLUT1-cre mice injected with the HACB2-AAV, imparted neuroprotective effects against acute seizures, we subjected AAV-injected mice to intraperitoneal injections of PTZ (40 mg/kg), which induced seizures reliably in naive animals with minimal mortality. Three weeks after bilateral CA1 injection with HACB2-AAV ($n = 15$ mice) or a control EGFP-AAV ($n = 12$ mice), we assessed seizures along a modified Racine scale after a single dose of PTZ. The mice injected with the HACB2-AAV displayed lower cumulative seizure scores over the 30 min observed, compared with the EGFP-AAV control mice (Kolmogorov–Smirnov test, $p < 0.001$; Fig. 5A). HACB2-AAV-injected mice were less likely to have higher intensity seizures after PTZ compared with the control mice (Fisher’s exact, $p = 0.020$, $p = 0.019$, and $p = 0.002$; seizure scores 4, 5, and 6, respectively; Fig. 5B). When comparing the onset latency to the first seizure of each intensity score (Fig. 5C), we found an increased latency period for the HACB2-AAV mice for seizure scores 1 and 2 (CB: 216.1 ± 16.6 s, EGFP: 76.4 ± 2.6 s; and CB: 260.0 ± 22.4 s, EGFP: 83.3 ± 2.8 s; unpaired t test, $p = 0.031$ and $p = 0.042$, respectively). However, the increased latency times were not statistically significant at the higher seizure scores because of the low numbers of HACB2-AAV mice having high intensity seizures (note the diminishing number of data points in Fig. 5C).

Discussion

We evaluated the effects of overexpressing CB in specific neuron types in the adult dorsal hippocampus. While CBSH3+ splice variants are the far more abundantly expressed isoforms of CB (Harvey et al., 2004), they are autoinhibited in their ability to induce clustering of gephyrin, unless relieved by other postsynaptic proteins (Poulopoulos et al., 2009; Mayer et al., 2013; Soykan et

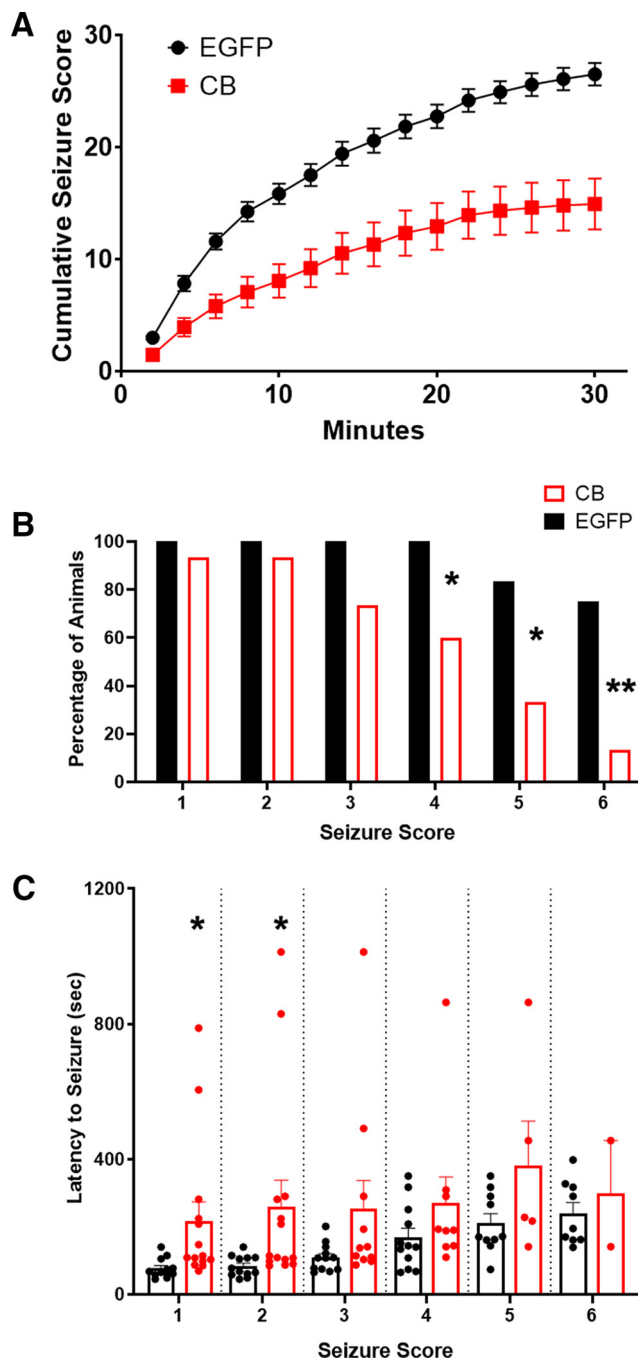


Figure 5. VGLUT1-IRES-cre mouse injected intrahippocampally with mCitrine-HACB2-AAV display lower susceptibility to PTZ-induced intense seizures. **A**, Seizures were scored along a modified Racine scale and a maximal seizure score assigned in 2-min bins, and average cumulative scores are presented. **B**, The percentage of animals that had a seizure at each intensity score. Asterisks indicate significance using Fisher’s exact test; * $p < 0.05$, ** $p < 0.01$. **C**, The average latency to the first seizure of each intensity was recorded. Error bars indicate SEM, and each dot represents one animal. Note that at higher intensity seizure scores, there are fewer mice that seize, particularly in the CB category. Most mice seize with lower intensities. Asterisks indicate significance using unpaired t test; * $p < 0.05$.

al., 2014). The constitutively active CBSH3- isoforms, however, are capable of inducing the accumulation of gephyrin and GABA_ARs at postsynaptic sites (Chiou et al., 2011; Tyagarajan et al., 2011; Fekete et al., 2017). We found that overexpression of CB2SH3- in hippocampal CA1 pyramidal neurons resulted in significantly increased CB, gephyrin and GABA_AR clustering in perisomatic regions (within SP). Overexpression of CB2SH3- in CA1 interneurons also resulted in increased CB expression, and larger perisomatic gephyrin and GABA_AR clusters. The increase in postsynaptic GABAergic receptors was accompanied by a significantly increased mIPSC amplitude and frequency. Overexpression of CB2SH3- in excitatory neurons in CA1 of the dorsal hippocampus also provided resilience against PTZ-induced seizures.

In CA1 pyramidal cells, overexpression of CB2SH3- resulted in an increase in gephyrin and GABA_AR cluster size. The majority of these large gephyrin clusters were apposed to VGAT terminals, indicating localization to GABAergic synapses. This is consistent with what has been seen in cultured hippocampal neurons transfected to overexpress CB2SH3- (Chiou et al., 2011; Tyagarajan et al., 2011; Körber et al., 2012) and in CB2SH3- transfected pyramidal neurons of the cerebral cortex of *in utero* electroporated (IUE) rats (Fekete et al., 2017). In HACB2-AAV transduced hippocampal pyramidal cells, the increase in amplitude of spontaneous mIPSCs further indicates an accumulation of GABA_ARs at the postsynapse.

Immunofluorescence revealed an increase in synaptic γ 2-containing GABA_ARs in SP, but not in SO or SR, despite CA1 pyramidal cells receiving 92% of their GABAergic synaptic input at their dendrites (Megias et al., 2001). Each cell compartment is typically innervated by different interneuron subtypes, with parvalbumin (PV)+ and cholecystokinin (CCK)+ basket cells providing the majority of GABAergic innervation to perisomatic regions (Miles et al., 1996; Salesse et al., 2011). In addition, PV+ chandelier cells almost exclusively innervate the axon initial segments of pyramidal cells, which lie at the border of SP and SO (Buhl et al., 1994). The increased GABA_AR γ 2 clustering in SP suggests that the perisomatic synapses, in particular, are strengthened by HACB2-AAV transduction, although the longer rise times of spontaneous mIPSCs raise the possibility of increased GABA_AR clustering at more distal synapses, or the addition of GABA_ARs of alternative compositions to the perisomatic synapses. At these synapses, GABA_ARs predominantly have α 1 β 3 γ 2 and α 2 β 3 γ 2 subunit composition (Nusser et al., 1996; Nyíri et al., 2001; Kasugai et al., 2010). The increase in postsynaptic gephyrin cluster size might attract extrasynaptic α 5 β 3 γ 2 GABA_ARs into the postsynapse. The α 5 β 3 γ 2 GABA_ARs are mostly extrasynaptic but can also be synaptically localized (Brüning et al., 2002; Christie et al., 2002; Schweizer et al., 2003; Alldred et al., 2005; Serwanski et al., 2006). The incorporation of α 5 β 3 γ 2 GABA_ARs into the synapse is consistent with the longer rise times and very slow deactivation of α 5 β 3 γ 2 GABA_ARs compared with α 1 β 3 γ 2 and α 2 β 3 γ 2 (Mortensen et al., 2012). In hippocampal pyramidal neurons, the α 5, α 2, and α 1 are the three most

abundant α GABA_AR subunits, in that order (Wisden et al., 1992; Fritschy and Mohler, 1995; Nusser et al., 1996; Brüning et al., 2002; Serwanski et al., 2006; Kasugai et al., 2010). Immunofluorescence revealed that the effects of HACB2-AAV on enhancing postsynaptic GABA_AR clustering are more subdued than the effects on gephyrin clustering. We attribute it to the fact that gephyrin clustering in these cells is largely concentrated on GABAergic synapses, while γ 2-containing GABA_ARs are both synaptic and extrasynaptic.

We did not observe any changes in density, MFI, or size of VGAT puncta, which is consistent with previous studies indicating that CB is not synaptogenic: knocking out CB in mice, while disruptive of gephyrin clusters in certain brain regions, does not affect presynaptic GABAergic innervation (Papadopoulos et al., 2007), nor does knock-down of CBSH3- or CBSH3+ isoforms (George et al., 2021) or overexpression of CB (Chiou et al., 2011; Fekete et al., 2017). Nevertheless, we observed a left-shift in interevent interval and increase in frequency of mIPSCs in CB2SH3- overexpressing cells. Since this is not accompanied by increased presynaptic GABAergic innervation, as shown by VGAT immunofluorescence, the result is consistent with an increased probability of spontaneous vesicular GABA release from presynaptic terminals onto HACB2-AAV-transduced cells. Therefore, increased postsynaptic clustering of gephyrin/GABA_ARs seems to have a transsynaptic effect on spontaneous GABA release. PV+ and CCK+ basket cells in the hippocampus have distinct mechanisms for modulating presynaptic release. While CCK+ basket cell terminals are covered in cannabinoid and GABA_BRs (Marsicano and Lutz, 1999; Sloviter et al., 1999; Liu et al., 2019), M₂ muscarinic and μ -opioid receptors modulate activity at PV+ basket cell terminals (Hájos et al., 1998; Drake and Milner, 2006; Freund and Katona, 2007). The increase in spontaneous mIPSC frequency is contrary to the decreased frequency observed in pyramidal cells of rat cerebral cortex transfected by IUE to overexpress CB2SH3- (Fekete et al., 2017). This difference could be attributed to: (1) being neurons in different brain areas innervated by different interneurons; or (2) the IUE study involved CB2SH3- overexpression in a sparse population of pyramidal neurons in cerebral cortex since embryonic age, which has the potential for altering synaptic function in the adult.

The possibility of enhancing synaptic GABAergic neurotransmission in hippocampal circuits is of particular interest in regards to circuits in which there is an excitation/inhibition imbalance. In the current study, we used the chemoconvulsant PTZ to induce acute seizures. The mechanism of action for PTZ is not well understood, but it has been demonstrated to cause calcium and sodium influx in neurons, thereby resulting in depolarization (Papp et al., 1987). PTZ been used to model acute seizures with a single dose, and to study epileptogenesis in chemical kindling models with multiple subthreshold doses. In VGLUT1-cre mice injected with HACB2-AAV, latency to PTZ-induced seizure events was increased and mice were less likely to develop severe seizures, thereby demonstrating that enhancing the strength of GABAergic synaptic inhibition through HACB2-AAV transduction provided

protection against convulsions. Our results bring attention to CB as a possible target for therapeutic intervention. They suggest that enhancing CB expression or enhancing the activity of existing endogenous CB in a selected population of hyperactive hippocampal neurons may decrease their activity and prove useful in ameliorating seizures originating in hippocampal structures such as temporal lobe epilepsy.

In VGAT-cre mice, we quantified interneurons with soma residing within the SP. While the majority of these cells are PV+ basket cells, there are many additional interneuron types whose soma can be found within or immediately adjacent to the SP, including CCK+ basket cells, PV+ bistratified or chandelier cells, ivy cells, and vasointestinal active peptide (VIP)+ type 1 or three interneuron selective interneurons (Klausberger, 2009; Pelkey et al., 2017). Many additional interneuron types were transduced in the SO and SR that may be bistratified cells, oriens-lacunosum moleculare cells, or CCK+/VIP+ basket cells (Sik et al., 1995; Baude et al., 2007). The vast majority of boutons from pyramidal layer interneurons terminate on pyramidal cells within the SP or onto the soma of other basket cells or bistratified cells within the SP (Sik et al., 1995; Földy et al., 2010). CB may be differentially expressed between various interneuron types. It has been shown that PV+ interneurons in the hippocampus and cerebral cortex contain higher levels of endogenous CB (Arhgef9) transcripts and protein than other interneurons (Paul et al., 2017; George et al., 2021). We found that transduction with the HACB2-AAV resulted in increased expression of CB in transduced interneurons compared with control EGFP-AAV transduced interneurons.

Transduction of interneurons with HACB2-AAV resulted in roughly two-fold increases in both size and density of perisomatic gephyrin and modest increases in perisomatic GABA_AR clusters. This effect was not accompanied by any changes to size, density, or MFI of presynaptic VGAT input onto the soma, indicating that CBSH3- overexpression does not recruit additional GABAergic innervation to these cells. To maintain consistency in our analysis, we restricted ourselves to quantification in cells within the center of SP. However, nearly every HACB2-AAV-transduced CA1 interneuron, including those in SO and on the perimeter of SR, displayed a noticeably strong perisomatic ring of gephyrin clusters. This was rarely seen in non-transduced interneurons of the contralateral CA1 or in EGFP-AAV-transduced CA1 interneurons. However, strong diffuse or punctate extrasynaptic immunoreactivity with the GABA_AR γ 2 antibody was frequently seen in CA1 interneurons, in VGAT-cre as well as VGLUT1-cre mice, and in both HACB2-AAV and EGFP-AAV injected and non-injected hemispheres, indicating that the γ 2-containing GABA_ARs in interneurons are not only synaptic but also extrasynaptic.

The results of HACB2-AAV injection in VGAT-cre mice indicates that our approach can also be used for targeting GABAergic interneurons for the conditional overexpression of CBSH3-. However, because of the heterogeneity of the transduced interneurons and the diversity of synaptic inhibitory GABAergic inputs from other interneurons,

the VGAT-cre mice are not adequate to properly interrogate the functional outcomes, which would be hard if not impossible to interpret. Instead, CB overexpression can be tailored to target-specific classes of interneurons in the hippocampus or any region of the brain by using selected interneuron-type-specific cre-driver mouse lines (i.e., PV-cre, CCK-cre, Calbindin2-cre, SOM-Cre, and VIP-cre among others). These future studies are beyond the scope of this article.

Enhancement of inhibitory synapses have also been accomplished by overexpression of NL2, a cell-adhesion molecule found selectively at inhibitory postsynapses which interacts with and activates CBSH3+ (Pouloupoulos et al., 2009; Soykan et al., 2014). It has also been demonstrated to interact with gephyrin and CB forming a tripartite complex at GABAergic synapses with GABA_AR- γ 2 and the transmembrane GABA_AR accessory protein LHFPL4 or GARLH (Varoqueaux et al., 2004; Davenport et al., 2017; Yamasaki et al., 2017). Two studies have investigated AAV-mediated overexpression of NL2 in the hippocampus. In one study, overexpression of NL2 results in increased gephyrin clusters and VGAT+ puncta by confocal microscopy immunofluorescence and an increase in the gephyrin, VGAT and GABA_AR- γ 2 subunit protein expression by western blot, suggesting a strengthening inhibitory synapses in the transduced neurons (Van Zandt et al., 2019). In the other study, increased NL2 expression leads to increased mRNA levels for GAD65, but no increase in neurexin-1, gephyrin, or GAD67 mRNAs (Kohl et al., 2013). Interestingly, the two AAV-mediated NL2-overexpression studies also revealed alterations to behavior, notably, reductions in social aggression and dominance behaviors but also diminished preference for social novelty. In another study, overexpression of NL2 in cortical pyramidal neurons after *in utero* electroporation shows an increase in VGAT which were associated to gephyrin clusters (Fekete et al., 2015). An increase in VGAT, but no change in gephyrin was reported in transgenic animals overexpressing NL2 (Hines et al., 2008). In the same study, it was determined that pyramidal neurons in the prefrontal cortex of these transgenic mice had increased mIPSC frequency but showed no effect on the amplitude of mIPSCs (Hines et al., 2008; Fekete et al., 2015). It is worth noting that in the two AAV-NL2 studies, NL2 was simultaneously overexpressed in both glutamatergic and GABAergic neurons. The NL2 overexpression studies strongly suggest that NL2 overexpression in neurons enhances GABAergic synaptic transmission and that if targeted to specific neurons might also be effective for seizure suppression.

The HACB2-AAV and described methodology can be generally applied for selective *in vivo* enhancement of GABAergic synaptic transmission in any neuronal type and brain region, by using the expanding collection of available Cre-driver mouse lines. Moreover, our DIO-AAV could also be used for the overexpression of CBSH3- in selected types of neurons in wild-type non-transgenic animal species besides mouse, by co-injecting it with another AAV carrying Cre-recombinase under the control of a neuron-type-specific modified promoter. This has been

accomplished in rat and monkey (Mikhailova et al., 2016; Stauffer et al., 2016; Zalocusky et al., 2016).

References

- Aarabi M, Kessler E, Madan-Khetarpal S, Surti U, Bellissimo D, Rajkovic A, Yatsenko SA (2019) Autism spectrum disorder in females with ARHGEF9 alterations and a random pattern of X chromosome inactivation. *Eur J Med Genet* 62:239–242.
- Aldred MJ, Mulder-Rosi J, Lingenfelter SE, Chen G, Luscher B (2005) Distinct gamma2 subunit domains mediate clustering and synaptic function of postsynaptic GABAA receptors and gephyrin. *J Neurosci* 25:594–603.
- Baude A, Bleasdale C, Dalezios Y, Somogyi P, Klausberger T (2007) Immunoreactivity for the GABAA receptor alpha1 subunit, somatostatin and Connexin36 distinguishes axoaxonic, basket, and bis-tratified interneurons of the rat hippocampus. *Cereb Cortex* 17:2094–2107.
- Bhat G, LaGrave D, Millson A, Herriges J, Lamb AN, Matalon R (2016) Xq11.1-11.2 deletion involving ARHGEF9 in a girl with autism spectrum disorder. *Eur J Med Genet* 59:470–473.
- Brüning I, Scotti E, Sidler C, Fritschy JM (2002) Intact sorting, targeting, and clustering of gamma-aminobutyric acid A receptor subtypes in hippocampal neurons in vitro. *J Comp Neurol* 443:43–55.
- Buhl EH, Halasy K, Somogyi P (1994) Diverse sources of hippocampal unitary inhibitory postsynaptic potentials and the number of synaptic release sites. *Nature* 368:823–828.
- Charych EI, Yu W, Miralles CP, Serwanski DR, Li X, Rubio M, De Blas AL (2004a) The brefeldin A-inhibited GDP/GTP exchange factor 2, a protein involved in vesicular trafficking, interacts with the beta subunits of the GABA receptors. *J Neurochem* 90:173–189.
- Charych EI, Yu W, Li R, Serwanski DR, Miralles CP, Li X, Yang BY, Pinal N, Walikonis R, De Blas AL (2004b) A four PDZ domain-containing splice variant form of GRIP1 is localized in GABAergic and glutamatergic synapses in the brain. *J Biol Chem* 279:38978–38990.
- Chiou TT, Bonhomme B, Jin H, Miralles CP, Xiao H, Fu Z, Harvey RJ, Harvey K, Vicini S, De Blas AL (2011) Differential regulation of the postsynaptic clustering of gamma-aminobutyric acid type A (GABAA) receptors by collybistin isoforms. *J Biol Chem* 286:22456–22468.
- Chiou TT, Long P, Schumann-Gillett A, Kanamarlapudi V, Haas SA, Harvey K, O'Mara ML, De BA, Kalscheuer VM, Harvey RJ (2019) Mutation p.R356Q in the collybistin phosphoinositide binding site is associated With mild intellectual disability. *Front Mol Neurosci* 12:60.
- Christie SB, De Blas AL (2003) GABAergic and glutamatergic axons innervate the axon initial segment and organize GABA(A) receptor clusters of cultured hippocampal pyramidal cells. *J Comp Neurol* 456:361–374.
- Christie SB, Li R-W, Miralles CP, Riquelme R, Yang BY, Charych E, Wendou Y, Daniels SB, Cantino ME, De Blas AL (2002) Synaptic and extrasynaptic GABAA receptor and gephyrin clusters. *Prog Brain Res* 136:157–180.
- Davenport EC, Pendolino V, Kontou G, McGee TP, Sheehan DF, López-Doménech G, Farrant M, Kittler JT (2017) An essential role for the tetraspanin LHFPL4 in the cell-type-specific targeting and clustering of synaptic GABA_A receptors. *Cell Rep* 21:70–83.
- Drake CT, Milner TA (2006) Mu opioid receptors are extensively co-localized with parvalbumin, but not somatostatin, in the dentate gyrus. *Neurosci Lett* 403:176–180.
- Fekete CD, Chiou TT, Miralles CP, Harris RS, Fiondella CG, Loturco JJ, De Blas AL (2015) In vivo clonal overexpression of neuroligin 3 and neuroligin 2 in neurons of the rat cerebral cortex: differential effects on GABAergic synapses and neuronal migration. *J Comp Neurol* 523:1359–1378.
- Fekete CD, Goz RU, Dinallo S, Miralles CP, Chiou TT, Bear J Jr, Fiondella CG, LoTurco JJ, De Blas AL (2017) In vivo transgenic expression of collybistin in neurons of the rat cerebral cortex. *J Comp Neurol* 525:1291–1311.
- Földy C, Lee SH, Morgan RJ, Soltesz I (2010) Regulation of fast-spiking basket cell synapses by the chloride channel ClC-2. *Nat Neurosci* 13:1047–1049.
- Freund TF, Katona I (2007) Perisomatic inhibition. *Neuron* 56:33–42.
- Fritschy JM, Mohler H (1995) GABAA-receptor heterogeneity in the adult rat brain: differential regional and cellular distribution of seven major subunits. *J Comp Neurol* 359:154–194.
- George S, Bear J Jr, Taylor MJ, Kanamalla K, Fekete CD, Chiou TT, Miralles CP, Papadopoulos T, De Blas AL (2021) Collybistin SH3-protein isoforms are expressed in the rat brain promoting gephyrin and GABA-A receptor clustering at GABAergic synapses. *J Neurochem* 157:1032–1051.
- Grosskreutz Y, Hermann A, Kins S, Fuhrmann JC, Betz H, Kneussel M (2001) Identification of a gephyrin-binding motif in the GDP/GTP exchange factor collybistin. *Biol Chem* 382:1455–1462.
- Hájos N, Papp EC, Acsády L, Levey AI, Freund TF (1998) Distinct interneuron types express m2 muscarinic receptor immunoreactivity on their dendrites or axon terminals in the hippocampus. *Neuroscience* 82:355–376.
- Harvey K, Duguid IC, Aldred MJ, Beatty SE, Ward H, Keep NH, Lingenfelter SE, Pearce BR, Lundgren J, Owen MJ, Smart TG, Luscher B, Rees MI, Harvey RJ (2004) The GDP-GTP exchange factor collybistin: an essential determinant of neuronal gephyrin clustering. *J Neurosci* 24:5816–5826.
- Hines RM, Wu L, Hines DJ, Steenland H, Mansour S, Dahlhaus R, Singaraja RR, Cao X, Sammler E, Hormuzdi SG, Zhuo M, El-Husseini A (2008) Synaptic imbalance, stereotypies, and impaired social interactions in mice with altered neuroligin 2 expression. *J Neurosci* 28:6055–6067.
- Jin H, Chiou TT, Serwanski DR, Miralles CP, Pinal N, De Blas AL (2014) Ring finger protein 34 (RNF34) interacts with and promotes gamma-aminobutyric acid type-A receptor degradation via ubiquitination of the gamma2 subunit. *J Biol Chem* 289:29420–29436.
- Kalscheuer VM, Musante L, Fang C, Hoffmann K, Fuchs C, Carta E, Deas E, Venkateswarlu K, Menzel C, Ullmann R, Tommerup N, Dalprà L, Tzschach A, Selicorni A, Lüscher B, Ropers HH, Harvey K, Harvey RJ (2009) A balanced chromosomal translocation disrupting ARHGEF9 is associated with epilepsy, anxiety, aggression, and mental retardation. *Hum Mutat* 30:61–68.
- Kasugai Y, Swinny JD, Roberts JD, Dalezios Y, Fukazawa Y, Sieghart W, Shigemoto R, Somogyi P (2010) Quantitative localisation of synaptic and extrasynaptic GABAA receptor subunits on hippocampal pyramidal cells by freeze-fracture replica immunolabelling. *Eur J Neurosci* 32:1868–1888.
- Khan ZU, Gutiérrez A, De Blas AL (1994) Short and long form gamma 2 subunits of the GABAA/benzodiazepine receptors. *J Neurochem* 63:1466–1476.
- Kins S, Betz H, Kirsch J (2000) Collybistin, a newly identified brain-specific GEF, induces submembrane clustering of gephyrin. *Nat Neurosci* 3:22–29.
- Klausberger T (2009) GABAergic interneurons targeting dendrites of pyramidal cells in the CA1 area of the hippocampus. *Eur J Neurosci* 30:947–957.
- Klein KM, Pendziwiat M, Eilam A, Gilad R, Blatt I, Rosenow F, Kanaan M, Helbig I, Afawi Z; Israeli-Palestinian Epilepsy Family Consortium (2017) The phenotypic spectrum of ARHGEF9 includes intellectual disability, focal epilepsy and febrile seizures. *J Neurol* 264:1421–1425.
- Kneussel M, Brandstätter JH, Laube B, Stahl S, Müller U, Betz H (1999) Loss of postsynaptic GABA(A) receptor clustering in gephyrin-deficient mice. *J Neurosci* 19:9289–9297.
- Kohl C, Riccio O, Grosse J, Zanoletti O, Fournier C, Schmidt MV, Sandi C (2013) Hippocampal neuroligin-2 overexpression leads to reduced aggression and inhibited novelty reactivity in rats. *PLoS One* 8:e56871.
- Körber C, Richter A, Kaiser M, Schlicksupp A, Mükusch S, Kuner T, Kirsch J, Kuhse J (2012) Effects of distinct collybistin isoforms on

- the formation of GABAergic synapses in hippocampal neurons. *Mol Cell Neurosci* 50:250–259.
- Lesca G, Till M, Labalme A, Vallee D, Hugononq C, Philip N, Ederly P, Santaville D (2011) De novo Xq11.11 microdeletion including ARHGEF9 in a boy with mental retardation, epilepsy, macrosomia, and dysmorphic features. *Am J Med Genet A* 155A:1706–1711.
- Li RW, Yu W, Christie S, Miralles CP, Bai J, Loturco JJ, De Blas AL (2005a) Disruption of postsynaptic GABA receptor clusters leads to decreased GABAergic innervation of pyramidal neurons. *J Neurochem* 95:756–770.
- Li RW, Yu W, Christie S, Miralles CP, Bai J, Loturco JJ, De Blas AL (2005b) Disruption of postsynaptic GABA receptor clusters leads to decreased GABAergic innervation of pyramidal neurons. *J Neurochem* 95:756–770.
- Li X, Serwanski DR, Miralles CP, Bahr BA, De Blas AL (2007) Two pools of Triton X-100-insoluble GABA(A) receptors are present in the brain, one associated to lipid rafts and another one to the postsynaptic GABAergic complex. *J Neurochem* 102:1329–1345.
- Li Y, Serwanski DR, Miralles CP, Fiondella CG, Loturco JJ, Rubio ME, De Blas AL (2010) Synaptic and nonsynaptic localization of protocadherin-gammaC5 in the rat brain. *J Comp Neurol* 518:3439–3463.
- Li Y, Xiao H, Chiou TT, Jin H, Bonhomme B, Miralles CP, Pinal N, Ali R, Chen WV, Maniatis T, De Blas AL (2012) Molecular and functional interaction between protocadherin-gammaC5 and GABAA receptors. *J Neurosci* 32:11780–11797.
- Lionel AC, Vaags AK, Sato D, Gazzellone MJ, Mitchell EB, Chen HY, Costain G, Walker S, Egger G, Thiruvahindrapuram B, Merico D, Prasad A, Anagnostou E, Fombonne E, Zwaigenbaum L, Roberts W, Szatmari P, Fernandez BA, Georgieva L, Brzustowicz LM, et al. (2013) Rare exonic deletions implicate the synaptic organizer Gephyrin (GPHN) in risk for autism, schizophrenia and seizures. *Hum Mol Genet* 22:2055–2066.
- Liu Y, Yang XJ, Xia H, Tang CM, Yang K (2019) GABA releases from parvalbumin-expressing and unspecific GABAergic neurons onto CA1 pyramidal cells are differentially modulated by presynaptic GABA(B) receptors in mouse hippocampus. *Biochem Biophys Res Commun* 520:449–452.
- Long P, May MM, James VM, Granno S, Johnson JP, Tarpey P, Stevenson RE, Harvey K, Schwartz CE, Harvey RJ (2015) Missense mutation R338W in ARHGEF9 in a family with X-linked intellectual disability with variable macrocephaly and macro-orchidism. *Front Mol Neurosci* 8:83.
- Ludolphs M, Schneeberger D, Soykan T, Schäfer J, Papadopoulos T, Brose N, Schindelin H, Steinem C (2016) Specificity of collybistin-phosphoinositide interactions: impact of the individual protein domains. *J Biol Chem* 291:244–254.
- Lüttjohann A, Fabene PF, van Luijtelaar G (2009) A revised Racine's scale for PTZ-induced seizures in rats. *Physiol Behav* 98:579–586.
- Marco EJ, Abidi FE, Bristow J, Dean WB, Cotter P, Jeremy RJ, Schwartz CE, Sherr EH (2008) ARHGEF9 disruption in a female patient is associated with X linked mental retardation and sensory hyperarousal. *J Med Genet* 45:100–105.
- Marsicano G, Lutz B (1999) Expression of the cannabinoid receptor CB1 in distinct neuronal subpopulations in the adult mouse forebrain. *Eur J Neurosci* 11:4213–4225.
- Mayer S, Kumar R, Jaiswal M, Soykan T, Ahmadian MR, Brose N, Betz H, Rhee JS, Papadopoulos T (2013) Collybistin activation by GTP-TC10 enhances postsynaptic gephyrin clustering and hippocampal GABAergic neurotransmission. *Proc Natl Acad Sci USA* 110:20795–20800.
- Megias M, Emri Z, Freund TF, Gulyás AI (2001) Total number and distribution of inhibitory and excitatory synapses on hippocampal CA1 pyramidal cells. *Neuroscience* 102:527–540.
- Mikhailova MA, Bass CE, Grinevich VP, Chappell AM, Deal AL, Bonin KD, Weiner JL, Gainetdinov RR, Budygin EA (2016) Optogenetically-induced tonic dopamine release from VTA-nucleus accumbens projections inhibits reward consummatory behaviors. *Neuroscience* 333:54–64.
- Miles R, Tóth K, Gulyás AI, Hájos N, Freund TF (1996) Differences between somatic and dendritic inhibition in the hippocampus. *Neuron* 16:815–823.
- Miralles CP, Taylor MJ, Bear J Jr, Fekete CD, George S, Li Y, Bonhomme B, Chiou TT, De Blas AL (2020) Expression of protocadherin- γ C4 protein in the rat brain. *J Comp Neurol* 528:840–864.
- Mortensen M, Patel B, Smart T (2012) GABA potency at GABAA receptors found in synaptic and extrasynaptic zones. *Front Cell Neurosci* 6:1.
- Mukherjee J, Kretschmannova K, Gouzer G, Maric HM, Ramsden S, Tretter V, Harvey K, Davies PA, Triller A, Schindelin H, Moss SJ (2011) The residence time of GABA(A)Rs at inhibitory synapses is determined by direct binding of the receptor α 1 subunit to gephyrin. *J Neurosci* 31:14677–14687.
- Nathanson AJ, Zhang Y, Smalley JL, Ollerhead TA, Rodriguez Santos MA, Andrews PM, Wobst HJ, Moore YE, Brandon NJ, Hines RM, Davies PA, Moss SJ (2019) Identification of a core amino acid motif within the α subunit of GABA $_A$ Rs that promotes inhibitory synaptogenesis and resilience to seizures. *Cell Rep* 28:670–681.e8.
- Nusser Z, Sieghart W, Benke D, Fritschy JM, Somogyi P (1996) Differential synaptic localization of two major gamma-aminobutyric acid type A receptor alpha subunits on hippocampal pyramidal cells. *Proc Natl Acad Sci USA* 93:11939–11944.
- Nyiri G, Freund TF, Somogyi P (2001) Input-dependent synaptic targeting of alpha(2)-subunit-containing GABA(A) receptors in synapses of hippocampal pyramidal cells of the rat. *Eur J Neurosci* 13:428–442.
- Papadopoulos T, Korte M, Eulenburg V, Kubota H, Retiounskaia M, Harvey RJ, Harvey K, O'Sullivan GA, Laube B, Hülsmann S, Geiger JR, Betz H (2007) Impaired GABAergic transmission and altered hippocampal synaptic plasticity in collybistin-deficient mice. *EMBO J* 26:3888–3899.
- Papadopoulos T, Eulenburg V, Reddy-Alla S, Mansuy IM, Li Y, Betz H (2008) Collybistin is required for both the formation and maintenance of GABAergic postsynapses in the hippocampus. *Mol Cell Neurosci* 39:161–169.
- Papadopoulos T, Schemm R, Grubmüller H, Brose N (2015) Lipid binding defects and perturbed synaptogenic activity of a Collybistin R290H mutant that causes epilepsy and intellectual disability. *J Biol Chem* 290:8256–8270.
- Papadopoulos T, Rhee HJ, Subramanian D, Paraskevopoulou F, Mueller R, Schultz C, Brose N, Rhee JS, Betz H (2017) Endosomal phosphatidylinositol 3-phosphate promotes gephyrin clustering and GABAergic neurotransmission at inhibitory postsynapses. *J Biol Chem* 292:1160–1177.
- Papp A, Fehér O, Erdélyi L (1987) The ionic mechanism of the pentylenetetrazol convulsions. *Acta Biol Hung* 38:349–361.
- Paul A, Crow M, Raudales R, He M, Gillis J, Huang ZJ (2017) Transcriptional architecture of synaptic communication delineates GABAergic neuron identity. *Cell* 171:522–539.e20.
- Pelkey KA, Chittajallu R, Craig MT, Tricoire L, Wester JC, McBain CJ (2017) Hippocampal GABAergic inhibitory interneurons. *Physiol Rev* 97:1619–1747.
- Pouloupoulos A, Aramuni G, Meyer G, Soykan T, Hoon M, Papadopoulos T, Zhang M, Paarmann I, Fuchs C, Harvey K, Jedlicka P, Schwarzacher SW, Betz H, Harvey RJ, Brose N, Zhang W, Varoqueaux F (2009) Neuroligin 2 drives postsynaptic assembly at perisomatic inhibitory synapses through gephyrin and collybistin. *Neuron* 63:628–642.
- Racine RJ (1972) Modification of seizure activity by electrical stimulation. II. Motor seizure. *Electroencephalogr Clin Neurophysiol* 32:281–294.
- Reddy-Alla S, Schmitt B, Birkenfeld J, Eulenburg V, Dutertre S, Böhringer C, Götz M, Betz H, Papadopoulos T (2010) PH-domain-driven targeting of collybistin but not Cdc42 activation is required for synaptic gephyrin clustering. *Eur J Neurosci* 31:1173–1184.

- Saiepour L, Fuchs C, Patrizi A, Sassoè-Pognetto M, Harvey RJ, Harvey K (2010) Complex role of collybistin and gephyrin in GABAA receptor clustering. *J Biol Chem* 285:29623–29631.
- Salesse C, Mueller CL, Chamberland S, Topolnik L (2011) Age-dependent remodelling of inhibitory synapses onto hippocampal CA1 oriens-lacunosum moleculare interneurons. *J Physiol* 589:4885–4901.
- Schweizer C, Balsiger S, Bluethmann H, Mansuy IM, Fritschy JM, Mohler H, Luscher B (2003) The gamma 2 subunit of GABA(A) receptors is required for maintenance of receptors at mature synapses. *Mol Cell Neurosci* 24:442–450.
- Serwanski DR, Miralles CP, Christie SB, Mehta AK, Li X, De Blas AL (2006) Synaptic and nonsynaptic localization of GABAA receptors containing the alpha5 subunit in the rat brain. *J Comp Neurol* 499:458–470.
- Shimajima K, Sugawara M, Shichiji M, Mukaida S, Takayama R, Imai K, Yamamoto T (2011) Loss-of-function mutation of collybistin is responsible for X-linked mental retardation associated with epilepsy. *J Hum Genet* 56:561–565.
- Sik A, Penttonen M, Ylinen A, Buzsáki G (1995) Hippocampal CA1 interneurons: an in vivo intracellular labeling study. *J Neurosci* 15:6651–6665.
- Singh P, Singh D, Goel RK (2016) Protective effect on phenytoin-induced cognition deficit in pentylenetetrazol kindled mice: a repertoire of *Glycyrrhiza glabra* flavonoid antioxidants. *Pharm Biol* 54:1209–1218.
- Sloviter RS, Ali-Akbarian L, Elliott RC, Bowery BJ, Bowery NG (1999) Localization of GABA(B) (R1) receptors in the rat hippocampus by immunocytochemistry and high resolution autoradiography, with specific reference to its localization in identified hippocampal interneuron subpopulations. *Neuropharmacology* 38:1707–1721.
- Soykan T, Schneeberger D, Tria G, Buechner C, Bader N, Svergun D, Tessmer I, Pouloupoulos A, Papadopoulos T, Varoqueaux F, Schindelin H, Brose N (2014) A conformational switch in collybistin determines the differentiation of inhibitory postsynapses. *EMBO J* 33:2113–2133.
- Stauffer WR, Lak A, Yang A, Borel M, Paulsen O, Boyden ES, Schultz W (2016) Dopamine neuron-specific optogenetic stimulation in rhesus macaques. *Cell* 166:1564–1571.e6.
- Tretter V, Jacob TC, Mukherjee J, Fritschy JM, Pangalos MN, Moss SJ (2008) The clustering of GABA(A) receptor subtypes at inhibitory synapses is facilitated via the direct binding of receptor alpha 2 subunits to gephyrin. *J Neurosci* 28:1356–1365.
- Tretter V, Kerschner B, Milenkovic I, Ramsden SL, Ramerstorfer J, Saiepour L, Maric HM, Moss SJ, Schindelin H, Harvey RJ, Sieghart W, Harvey K (2011) Molecular basis of the gamma-amino-butyric acid A receptor alpha3 subunit interaction with the clustering protein gephyrin. *J Biol Chem* 286:37702–37711.
- Tyagarajan SK, Ghosh H, Harvey K, Fritschy J-M (2011) Collybistin splice variants differentially interact with gephyrin and Cdc42 to regulate gephyrin clustering at GABAergic synapses. *J Cell Sci* 124:2786–2796.
- Van Zandt M, Weiss E, Almyasheva A, Lipior S, Maisel S, Naegele JR (2019) Adeno-associated viral overexpression of neuroligin 2 in the mouse hippocampus enhances GABAergic synapses and impairs hippocampal-dependent behaviors. *Behav Brain Res* 362:7–20.
- Varoqueaux F, Jamain S, Brose N (2004) Neuroligin 2 is exclusively localized to inhibitory synapses. *Eur J Cell Biol* 83:449–456.
- Wang JY, Zhou P, Wang J, Tang B, Su T, Liu XR, Li BM, Meng H, Shi YW, Yi YH, He N, Liao WP (2018) ARHGEF9 mutations in epileptic encephalopathy/intellectual disability: toward understanding the mechanism underlying phenotypic variation. *Neurogenetics* 19:9–16.
- Wisden W, Laurie DJ, Monyer H, Seeburg PH (1992) The distribution of 13 GABAA receptor subunit mRNAs in the rat brain. I. Telencephalon, diencephalon, mesencephalon. *J Neurosci* 12:1040–1062.
- Yamasaki T, Hoyos-Ramirez E, Martenson JS, Morimoto-Tomita M, Tomita S (2017) GARLH family proteins stabilize GABA(A) receptors at synapses. *Neuron* 93:1138–1152.e6.
- Yao R, Zhang Y, Liu J, Wang J, Xu Y, Li N, Wang J, Yu T (2020) Clinical and molecular characterization of three novel ARHGEF9 mutations in patients with developmental delay and epilepsy. *J Mol Neurosci* 70:908–915.
- Yu W, Jiang M, Miralles CP, Li RW, Chen G, de Blas AL (2007) Gephyrin clustering is required for the stability of GABAergic synapses. *Mol Cell Neurosci* 36:484–500.
- Yu W, Charych EI, Serwanski DR, Li RW, Ali R, Bahr BA, De Blas AL (2008) Gephyrin interacts with the glutamate receptor interacting protein 1 isoforms at GABAergic synapses. *J Neurochem* 105:2300–2314.
- Zalocusky KA, Ramakrishnan C, Lerner TN, Davidson TJ, Knutson B, Deisseroth K (2016) Nucleus accumbens D2R cells signal prior outcomes and control risky decision-making. *Nature* 531:642–646.
- Zhu H, Pleil KE, Urban DJ, Moy SS, Kash TL, Roth BL (2014) Chemogenetic inactivation of ventral hippocampal glutamatergic neurons disrupts consolidation of contextual fear memory. *Neuropsychopharmacology* 39:1880–1892.